

Transmission Line Analogy for Relativistic Poynting-Flux Jets

R.V.E. Lovelace¹ & P.P. Kronberg^{2, 3}

¹*Department of Astronomy, Cornell University, Ithaca, NY 14853; email: lovelace@astro.cornell.edu*

²*Theoretical Division, Los Alamos Nat. Lab, Los Alamos, NM 87545 and*

³*Department of Physics, University of Toronto, ON M5S 1A7, Canada*

12 March 2019

ABSTRACT

Radio emission, polarization, and Faraday rotation maps of the radio jet of the galaxy 3C 303 have shown that one knot of this jet carries a *galactic*-scale electric current and that it is magnetically dominated. We develop the theory of magnetically dominated or Poynting-flux jets by making an analogy of a Poynting jet with a transmission line or waveguide carrying a net current and having a potential drop across it (from the jet’s axis to its radius) and a definite impedance which we derive. The electromagnetic energy flow in the jet is the jet impedance times the square of the jet current. The observed current in 3C 303 can be used to calculate the electromagnetic energy flow in this magnetically dominated jet. Time-dependent but not necessarily small perturbations of a Poynting-flux jet are described by the “telegrapher’s equations.” These predict the propagation speed of disturbances and the effective wave impedance for forward and backward propagating wave components. A localized disturbance of a Poynting jet gives rise to localized dissipation in the jet which may explain the enhanced synchrotron radiation in the knots of the 3C 303 jet, and also in the apparently stationary knot HST-1 in the jet near the nucleus of the nearby galaxy M87. For a relativistic Poynting jet on parsec scales, the reflected voltage wave from an inductive termination or load can lead to a backward propagating wave which breaks down the magnetic insulation of the jet giving $|\mathbf{E}|/|\mathbf{B}| \geq 1$. At the threshold for breakdown, $|\mathbf{E}|/|\mathbf{B}| = 1$, positive and negative particles are directly accelerated in the $\mathbf{E} \times \mathbf{B}$ direction which is approximately along the jet axis. Acceleration can occur up to Lorentz factors $\sim 10^7$. This particle acceleration mechanism is distinct from that in shock waves and that in magnetic field reconnection.

Key words: galaxies: jets — accretion discs — magnetic fields — acceleration of particles

1 INTRODUCTION

A fundamental open question of astrophysical jet models is how energy extracted from the accretion flow close to the black hole event horizon is transported along narrow jets to much larger distances. The total energy carried by the jets of active galaxies is estimated to be a non-negligible fraction of the massive black hole formation energy, $\sim 0.1M_{\text{bh}}c^2$ (Kronberg et al. 2001). The jets are initially highly relativistic and low-density and for this reason are *magnetically dominated* or *force-free*. In this limit a negligible fraction of the power is carried by the particle kinetic energy. That is, the energy outflow from the accretion disc is in the form of a collimated ‘Poynting-flux jet’ as proposed by Lovelace (1976) and subsequently studied in many papers (Benford 1978; Lovelace,

Wang, & Sulkanen 1987; Lynden-Bell 1996; Li, et al. 2001; Lovelace, et al. 2002; Lovelace & Romanova 2003; Nakamura et al. 2008).

An illustrative model for the formation of a relativistic Poynting jet is sketched in Fig. 1. A large scale magnetic field is assumed to thread the accretion disc. As a result of the differential rotation of the disc the field opens up giving a current outflow (or inflow) I along the spine of the jet of cylindrical radius r_J initially of the order of the Schwarzschild radius of the black hole (Lovelace & Romanova 2012). In this model the jet power comes from the accretion disc. The associated toroidal magnetic field B_ϕ is responsible for collimating the jet. An equal but opposite “return current” flows inward (or outward) at much larger radial distances

from the jet axis so that the net current outflow from the source is zero. Because the jet current and the return current have opposite signs they repel as a result of their magnetic interaction mediated by the toroidal magnetic field. This repulsion between the jet and its return current has been demonstrated in magnetohydrodynamic (MHD) simulations (Ustyugova et al. 2000; Nakamura et al. 2008). The energy flow in the jet is unidirectional and is carried predominantly by the Poynting flux $\hat{\mathbf{z}} \cdot (\mathbf{E} \times \mathbf{B})/\mu_0 = E_r \times B_\phi/\mu_0$ (MKS units), where E_r is the radial electric field of the jet. The power in the Poynting jet may come predominantly from the spin-down of the black hole (Blandford & Znajek 1977). This process, which depends on the presence of a magnetized accretion disc around the rotating black hole, has been studied with general relativistic MHD simulations (e.g., McKinney 2006; Beckwith, Hawley, & Krolik 2008; Tchekhovskoy, Narayan, & McKinney 2011).

Rotation measure gradients observed on parsec scales close to the nuclear central black hole have given evidence of electric current flow along the jets (Asada et al. 2002; Gabuzda, Murray, & Cronin 2004; Zavala & Taylor 2005). More recently, on a scale 10^4 times larger, radio emission, polarization, X-ray, and Faraday rotation maps of the radio jet of the galaxy 3C 303 have shown that one knot of this jet has a *galactic*-scale current of $\sim 3 \times 10^{18}$ Ampère flowing along the jet axis (Kronberg et al. 2011). The physical parameters of this knot derived from the observations indicate that the jet is magnetically dominated, that is, a Poynting jet. The existence of an axial current in this very large scale plasma flow suggests an electrical circuit analogy for the jet.

A further possible indication of a Poynting jet is the jet near the nucleus of the galaxy M87 which has been observed to have an apparently stationary but strongly time-dependent knot HST-1 in its jet (Biretta et al. 1999). This knot showed a dramatic peak in emission in about 2005.2 in the radio, optical, and X-ray bands (Harris et al. 2009).

In Sec. 2 we model a Poynting jet as a transmission line carrying a net axial current and having a potential drop across it. Further, we derive the transmission line impedance and the electromagnetic energy flow in the jet. Time-dependent but not necessarily small perturbations of a Poynting-flux jet (§2.2) are described by the ‘‘telegraphers’ equations’’ (Heaviside 1893). These are wave equations for the current and voltage across the line. The voltage and current consist in general of forward and backward propagating components. A localized irregularity of a Poynting jet (§2.3) can give rise to localized dissipation in the jet which may explain the enhanced synchrotron radiation in the knots of the 3C 303 jet and in the apparently stationary knot HST-1 in M87.

Secs. 2.4 & 2.5 consider highly relativistic Poynting jets on parsec-scales jets such as HST-1. In this case the reflected voltage wave from an inductive load can lead to a backward propagating wave which breaks down the magnetic insulation of the jet, giving $|\mathbf{E}|/|\mathbf{B}| \geq 1$. The threshold for this breakdown is $|\mathbf{E}|/|\mathbf{B}| = 1$. At this threshold, positive and negative particles are directly accelerated in the $\mathbf{E} \times \mathbf{B}$ direction which is approximately along the jet axis and can be accelerated to very high Lorentz factors. Sec. 3 gives conclusions of this work.

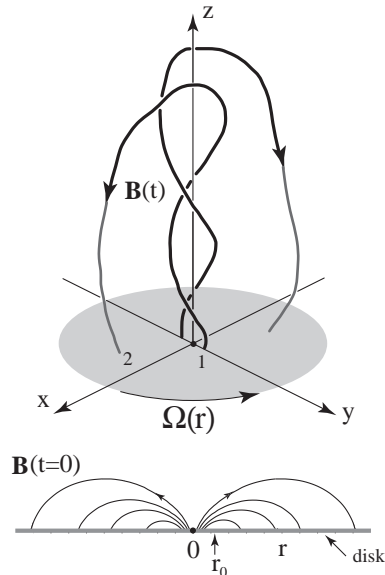


Figure 1. Sketch of the magnetic field configuration of a Poynting jet adapted from Lovelace and Romanova (2003). The bottom part of the figure shows the initial dipole-like magnetic field threading the disc which rotates at the angular rate $\Omega(r)$.

2 THEORY

In cylindrical (r, ϕ, z) coordinates with axisymmetry assumed, the magnetic field has the form $\mathbf{B} = \mathbf{B}_p + B_\phi \hat{\phi}$, with $\mathbf{B}_p = B_r \hat{r} + B_z \hat{z}$, and $B_r = -(1/r)(\partial\Psi/\partial z)$, and $B_z = (1/r)(\partial\Psi/\partial r)$. Here, $\Psi(r, z) \equiv rA_\phi(r, z)$ is the flux function. A simple form of this function is $\Psi(r, 0) = (1/2)r^2 B_0/[1 + 2(r/r_0)^3]$, where B_0 is the axial magnetic field strength in the center of the disc, and r_0 is the radius of the O -point of the magnetic field in the plane of the disc as indicated in Fig. 1. This Ψ is taken to apply for $r \geq 0$ even though it is not valid near the horizon of the black hole. The contribution from this region is negligible for the considered conditions where $(r_g/r_0)^2 \ll 1$, where $r_g \equiv GM/c^2$. For a corotating disc around a Kerr black hole the disc’s angular velocity viewed from a large distance is $\Omega = [c^3/(GM)]/[a_* + (r/r_g)^{3/2}]$, for $r > r_{ms}$ where r_{ms} is the innermost stable circular orbit and a_* is the spin parameter of the black hole with $0 \leq a_* < 1$.

At large distances from the disc ($z \gg r_0$) the flux function solution of the ‘force-free’ Grad-Shafranov equation is

$$\bar{\Psi} = \frac{\bar{r}^{4/3}}{[2\mathcal{R}(\Gamma^2 - 1)]^{2/3}}, \quad (1)$$

(Lovelace & Romanova 2003). The ‘force-free’ solution is applicable for conditions where the kinetic energy-density of the plasma is much less than the magnetic energy-density. Here Γ is the Lorentz factor of the jet, $\bar{r} \equiv r/r_0$, $\bar{\Psi} \equiv \Psi/\Psi_0$ with $\Psi_0 \equiv r_0^2 B_0/2$, and $\mathcal{R} \equiv r_0/r_g$. This dependence holds for $\bar{r}_1 \equiv [2(\Gamma^2 - 1)]^{1/2}/\mathcal{R} < \bar{r} < \bar{r}_2 \equiv [2\mathcal{R}(\Gamma^2 - 1)]^{1/2}/3^{3/4}$. At the inner radius \bar{r}_1 , $\bar{\Psi} = 1/\mathcal{R}^2$, which corresponds to the streamline which passes through the disc at a distance $r = r_g$. For $\bar{r} < \bar{r}_1$, we assume $\bar{\Psi} \propto \bar{r}^2$, which corresponds to $B_z = \text{const}$. At the outer radius \bar{r}_2 , $\bar{\Psi} = (\bar{\Psi})_{\text{max}} = 1/3$ which corresponds to the streamline which goes through the

disc near the O -point at $r = r_0$. Note that there is an appreciable range of radii if $\mathcal{R}^{3/2} \gg 1$.

For $\bar{r}_1 < r < \bar{r}_2$, the field components of the Poynting jet are

$$\bar{E}_r = -\sqrt{2} (\Gamma^2 - 1)^{1/2} \bar{B}_z, \quad \bar{B}_\phi = -\sqrt{2} \Gamma \bar{B}_z,$$

and

$$\bar{B}_z = \frac{2}{3} \frac{\bar{r}^{-2/3}}{[2\mathcal{R}(\Gamma^2 - 1)]^{2/3}}. \quad (2)$$

This electromagnetic field satisfies the radial force balance equation, $dB_z^2/dr + (1/r^2)d[r^2(B_\phi^2 - E_r^2)]/dr = 0$, for an axisymmetric, translationally-symmetric, and time-independent force-free field. Appendix A describes a different force-free jet model with electric and magnetic fields similar to those in a common coaxial transmission line.

At the jet radius r_2 , there is a boundary layer where the axial magnetic field changes from $B_z(r_2 - \varepsilon)$ to zero at $r_2 + \varepsilon$, where $\varepsilon \ll r_2$ is the half-width of this layer. The electric field changes from $E_r(r_2 - \varepsilon)$ to zero at $r_2 + \varepsilon$. The toroidal magnetic field changes from $B_\phi(r_2 - \varepsilon)$ to $B_\phi(r_2 + \varepsilon)$ where this change is fixed by the radial force balance. Thus for $r > r_2$, we have $E_r = 0$, $B_z = 0$, and $B_\phi = \sqrt{3}B_z(r_2 - \varepsilon)(r_2/r) = \sqrt{(3/2)}\Gamma^{-1}B_\phi(r_2 - \varepsilon)(r_2/r)$. Equivalently, $B_\phi(r_2 + \varepsilon)/B_\phi(r_2 - \varepsilon) = \sqrt{3/2}/\Gamma$.

The toroidal magnetic field for $r > r_2$ applies out to an ‘outer radius’ r_3 where the magnetic pressure of the jet’s toroidal magnetic field, $B_\phi^2(r_3)/8\pi = p_{\text{ex}}$, balances the external ram pressure $P_{\text{ex}} = p_{\text{ex}} + \rho_{\text{ex}}(dr_3/dt)^2$, where $p_{\text{ex}} = n_{\text{ex}}k_B T_{\text{ex}}$ is the kinetic pressure of the external intergalactic plasma and ρ_{ex} is its density. The outward propagation of the jet will be accompanied by the non-relativistic expansion of the outer radius, $dr_3/dt > 0$.

We take as the ‘jet current’ the axial current I_0 flowing along the jet core $r \leq r_2 - \varepsilon$. From Ampère’s law, $B_\phi(r_2) = -2I_0/(c r_2)$ or in convenient units, $B_\phi[\text{G}] = -I_0[\text{A}]/(5r[\text{cm}])$. The net current carried by the jet ($r \leq r_2 + \varepsilon$) is $I_{\text{net}} = \sqrt{3/2}\Gamma^{-1}I_0$.

Using equations (2), the energy flux carried by the Poynting jet can be expressed as

$$\dot{E}_J = \left[\frac{c}{2}, \frac{2\pi}{\mu_0} \right] \int_0^{r_2} r dr E_r B_\phi = \mathcal{Z}_0 I_0^2, \quad (3)$$

where the square bracket is for cgs or MKS units, and

$$\mathcal{Z}_0 = \frac{3}{c} \beta [\text{cgs}] = 90 \left(1 - \frac{1}{\Gamma^2} \right)^{1/2} \Omega [\text{MKS}], \quad (4)$$

where $\beta = U_z/c = (1 - \Gamma^{-2})^{1/2}$. Here, \mathcal{Z}_0 is the DC impedance of the Poynting jet. The conversion to MKS units is $c^{-1} \rightarrow (4\pi)^{-1}(\mu_0/\epsilon_0)^{1/2} = 30 \Omega$. Earlier, the impedance of a relativistic Poynting jet was estimated to be $\sim c^{-1}$ (Lovelace 1976).

We can apply these concepts to the jet in 3C 303 where the observed axial current in the E3 knot is 3.3×10^{18} A (Kronberg et al. 2011), Thus the electromagnetic energy flux is $\dot{E}_J \approx 8 \times 10^{45} \beta \text{ erg s}^{-1}$. This energy flux is much larger than the photon luminosity of the jet of $3.7 \times 10^{41} \text{ erg s}^{-1}$ integrated over 10^8 to 10^{17} Hz (Kronberg et al. 2011) assuming $\beta = U_z/c$ is not much smaller than unity. For the E3 knot the jet radius is $r_2 \approx 0.5 \text{ kpc}$ so that $B_\phi(r_2) \approx 0.4 \text{ mG}$. The E3 knot is about 17.7 kpc in projection from the galaxy nucleus.

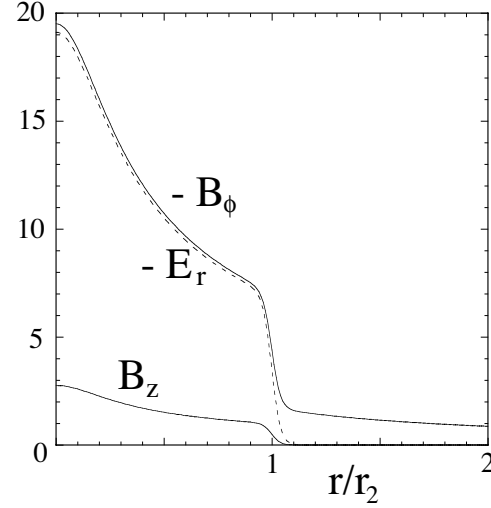


Figure 2. Radial dependence of the field components of a Poynting jet from equation (8). The inner jet radius is assumed to be $r_1 = 0.05r_2$, the boundary layer thickness is $\varepsilon = 0.01r_2$, and $\Gamma = 5$.

2.1 Transmission Line Analogy

Here, we interpret the Poynting flux jet in terms of a transmission line as proposed earlier by Lovelace & Ruchti (1983). The different physical quantities are measured in the ‘laboratory’ frame which is the rest frame of the plasma outside of the jet at $r \geq r_2$. The effective potential drop across the transmission line is taken to be

$$V_0 = -\frac{1}{2} r_0 \int_0^{r_2} d\bar{r} E_r(\bar{r}) = \frac{r_0}{3^{1/4}} \frac{B_0}{\sqrt{\mathcal{R}}}, \quad (5)$$

where the factor of one-half accounts for the fact that the transmission line does not consist of two conduction surfaces.

The axial current flow of the jet is

$$I_0 = -\frac{1}{2} c r_2 B_\phi(r_2) = \frac{V_0}{\mathcal{Z}_0}, \quad (6)$$

with \mathcal{Z}_0 given by equation (4). The units of equations (4) and (5) are cgs. In MKS units note that a current $I_0 = 3 \times 10^{18}$ A gives a voltage $V_0 = 2.7 \times 10^{20} \beta \text{ V}$. The energy of ions accelerated across this voltage is large enough to account for ultra high energy cosmic rays (Lovelace 1976; Biermann, Kang, & Ryu 2001; Ostrowski 2002).

There is a corresponding electric field energy per unit length of the jet which in MKS units is

$$w_E = \frac{\epsilon_0}{2} 2\pi \int_0^{r_2} r dr E_r^2 = \frac{1}{2} C V_0^2. \quad \text{Here, } C = \frac{4\pi\epsilon_0}{3} \quad (7)$$

is the capacitance per unit length in Farads per meter and $\epsilon_0 = 8.854 \times 10^{-12} \text{ F/m}$.

The magnetic energy per unit length of the jet in MKS units is

$$\begin{aligned} w_B &= \frac{\pi}{\mu_0} \int_0^{r_2} r dr (B_\phi^2 + B_z^2) + \frac{\pi}{\mu_0} \int_{r_2}^{r_3} r dr B_\phi^2 + \left(\frac{r_2}{r} \right)^2, \\ &= \frac{1}{2} L I_0^2. \end{aligned} \quad (8)$$

Here, $B_{\phi+}$ is the toroidal field at $r_2 + \varepsilon$. Carrying out the integrals we find

$$L = \frac{3\mu_0}{4\pi} \left[1 + \frac{1}{2\Gamma^2} + \frac{1}{2\Gamma^2} \ln \left(\frac{r_3}{r_2} \right) \right], \quad (9)$$

which is the inductance per unit length in Henrys per meter with $\mu_0 = 4\pi \times 10^{-7}$ H/m.

2.2 Telegraphers' Equations

Time and space (z -)dependent perturbations (not necessarily small) of a Poynting-flux jet are described by the Telegrapher's equations,

$$\frac{\partial \Delta V}{\partial t} = -\frac{1}{C} \frac{\partial \Delta I}{\partial z}, \quad \frac{\partial \Delta I}{\partial t} = -\frac{1}{L} \frac{\partial \Delta V}{\partial z}, \quad (10)$$

where $(\Delta V, \Delta I)$ represent deviations from the equilibrium values (V_0, I_0) (Heaviside 1893; Bergeron 1977; Samokhin 2010). The equations can be combined to give the wave equations

$$\left(\frac{\partial^2}{\partial t^2} - u_\varphi^2 \frac{\partial^2}{\partial z^2} \right) (\Delta V, \Delta I) = 0, \quad (11)$$

where

$$u_\varphi = \frac{1}{\sqrt{LC}} = c \left[1 + \frac{1}{2\Gamma^2} + \frac{1}{2\Gamma^2} \ln \left(\frac{r_3}{r_2} \right) \right]^{-1/2}, \quad (12)$$

is the phase velocity of the perturbation. The general solution of equation (10) is

$$\begin{aligned} \Delta V &= \Delta V_+(z - u_\varphi t) + \Delta V_-(z + u_\varphi t), \\ \Delta I &= \Delta I_+(z - u_\varphi t) + \Delta I_-(z + u_\varphi t), \end{aligned} \quad (13)$$

with

$$\Delta V_+ = Z \Delta I_+ \quad \text{and} \quad \Delta V_- = -Z \Delta I_-.$$

Here,

$$Z = \sqrt{\frac{L}{C}} = 90 \left[1 + \frac{1}{2\Gamma^2} + \frac{1}{2\Gamma^2} \ln \left(\frac{r_3}{r_2} \right) \right]^{1/2} \Omega \text{ [MKS]}, \quad (14)$$

is the wave impedance of the jet.

2.3 Irregularities in the Transmission Line:

A localized irregularity may appear in the transmission line due possibly to an instability at $t > 0$. The irregularity can be modeled as an extra impedance Z_ℓ or 'load' across the transmission line at $z = 0$. This impedance is considered to go from $Z_\ell(t < 0) = \infty$ to a constant value Z_ℓ for $t > 0$. In general Z_ℓ is complex with an imaginary component (reactance) which can be positive (capacitive) or negative (inductive). On either side of the discontinuity the line is assumed to have the impedance Z given by equation (14). On the upstream side of Z_ℓ ($z < 0$), the line voltage is $V_0 + \Delta V_-$, where ΔV_- is the backward propagating wave. The current on this part of the line is $I_0 + \Delta I_-$. There is no forward propagating wave for the conditions considered here. On the downstream side of Z_ℓ , the line voltage is $V_0 + \Delta V_t$ and the current is $I_0 + \Delta I_t$, where $(\Delta V_t, \Delta I_t = \Delta V_t/Z)$ represent the transmitted wave.

The standard conditions on the potential and current flow at Z_ℓ ($z = 0$) give $V_0 + \Delta V_- = V_0 + \Delta V_t$ and $I_0 + \Delta I_- =$

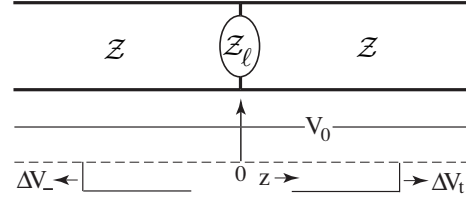


Figure 3. Diagram of an irregularity in the transmission line represented by the impedance $Z_\ell(t)$ where $Z_\ell(t < 0) = \infty$ and $Z_\ell(t > 0)$ is finite. Here, V_- the wave reflected off of Z_ℓ , V_t the transmitted wave, and V_0 is the line voltage for $t < 0$.

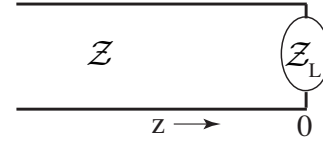


Figure 4. Diagram of a transmission line of impedance Z terminated by a load impedance Z_L with an inductive component.

$I_\ell + I_0 + \Delta I_t$, where $I_\ell = (V_0 + \Delta V_-)/Z_\ell$ is the current flow through Z_ℓ . In this way we find

$$\Delta V_- = \frac{-Z}{2Z_\ell + Z} V_0 = \Delta V_t. \quad (15)$$

Note that for $Z_\ell \rightarrow \infty$, both ΔV_- and ΔV_t tend to zero.

The power loss rate in the load Z_ℓ is

$$\dot{\mathcal{E}}_\ell = \frac{(V_0 + \Delta V_t)^2}{Z_\ell} = \frac{4Z_\ell}{(2Z_\ell + Z)^2} V_0^2. \quad (16)$$

We assume that this power goes into accelerating charged particles which in turn produce the observed synchrotron radiation. This power could account for the emission of the E3 knot of 3C 303 (Kronberg et al. 2011) and, on parsec scales, the emission of the HST-1 knot in the M87 jet (Biretta 1999).

The power $\dot{\mathcal{E}}_\ell$ is equal to the difference between the Poynting flux for $z < 0$,

$$S^- = (V_0 + \Delta V_-)(I_0 + \Delta I_-) = \frac{[V_0^2 - (\Delta V_-)^2]}{Z}, \quad (17)$$

and the Poynting flux for $z > 0$,

$$S^+ = (V_0 + \Delta V_t)(I_0 + \Delta I_t) = \frac{[V_0^2 + 2V_0\Delta V_t + (\Delta V_t)^2]}{Z}. \quad (18)$$

Using equation (17) we find that $S^- - S^+ = \dot{\mathcal{E}}_\ell$.

2.4 Magnetic Insulation

The Poynting jet is analogous to a magnetically insulated transmission line. In laboratory experiments magnetically insulated transmission lines involving crossed electric and magnetic fields are commonly used to transport pulses of high energy content onto small targets (e.g., Shope et al. 1978; Samokhin 2010). The condition for ‘‘magnetic insulation’’ of a planar gap of width d between a conducting cathode and anode with potential drop V_0 and initially filled

with a uniform magnetic field B_0 is $B_0^2 > (2V_e V_0 + V_0^2)d^{-2}$, where $V_e \equiv m_e c^2 / e \approx 5.14 \times 10^5$ V (Lovelace & Ott 1974; Ron, Mondelli, & Rostoker 1973).

In the astrophysical limit where $V_0 \gg V_e$, the condition for magnetic insulation is $|\mathbf{E}| < |\mathbf{B}|$ for the case where field components have the same radial dependence. If the power flow in the jet is *unidirectional*, as assumed in equations (2), then the condition for magnetic insulation is

$$\frac{|\mathbf{E}|}{|\mathbf{B}|} = \left(\frac{\Gamma^2 - 1}{\Gamma^2 + 1/2} \right)^{1/2} < 1 \quad \text{or} \quad \frac{V_0}{\mathcal{Z}_R I_0} < \left(1 + \frac{1}{2\Gamma^2} \right)^{1/2}, \quad (19)$$

where $\mathcal{Z}_R \equiv 90\Omega$ is a reference impedance. This inequality is always satisfied because the fields are time-independent and force-free ($\rho_e \mathbf{E} + \mathbf{J} \times \mathbf{B}/c = 0$).

Consider now the case where the power flow is *not unidirectional* and where the fields are time and space-dependent, i.e., $V(z, t) = \Delta V_+ + \Delta V_-$, $I(z, t) = \Delta I_+ + \Delta I_-$. We assume $\Gamma^2 \gg 1$ so that $(B_z/B_\phi)^2 = \mathcal{O}(\Gamma^{-2}) \ll 1$. To a first approximation the electric and magnetic fields correspond to those in a common transverse electric and magnetic (TEM) mode in a coaxial cable. Unlike a coaxial cable where the two conducting surfaces are separated by a dielectric, the Poynting jet has distributed charge and current densities. Because $|E_r/B_\phi| = V/(\mathcal{Z}I)$, the insulation condition $|\mathbf{E}| < |\mathbf{B}|$ can then be written as

$$\frac{V}{\mathcal{Z}I} < \mathcal{C}, \quad (20)$$

where $\mathcal{C} = 1 + \mathcal{O}(\Gamma^{-2})$ is a critical dimensionless number slightly larger than unity.

2.5 Consequences of Breakdown of Magnetic Insulation

Here we discuss conditions where the magnetic insulation breaks down in a localized region near the termination of a Poynting jet due to a load \mathcal{Z}_L which has an inductive component (Fig. 4). An essential condition for this to occur is that the wave propagation *not be unidirectional*. The load is assumed to be stationary or sub-relativistic in the laboratory frame owing to the ram pressure from the external plasma. The breakdown of magnetic insulation in laboratory transmission lines is discussed by Gordeev (1978).

The consequences of the breakdown can be dramatic: Nuclei can be accelerated to energies of the order of $eV \sim 3 \times 10^{20}$ eV while leptons may be accelerated to smaller energies owing to radiative losses and interactions with radiation. This value of the potential comes from the jet parameters deduced for 3C 303 with $\mathcal{Z} = 90\Omega$ (Kronberg et al. 2011). (Note that magnetic insulation breakdown can also occur *along* the jet due to the reflected wave from a localized region of increased series inductance along the transmission line.)

The voltage across the Poynting jet, $V = \Delta V_+ + \Delta V_-$, is assumed to be made up of an incident component ΔV_+ propagating along the jet channel with velocity u_ϕ and a reflected component ΔV_- with velocity $-u_\phi$. The corresponding jet current is $I = \Delta I_+ + \Delta I_-$. The spatial profile of the incident wave ΔV_+ is considered to be a smooth rise to a constant value (taken to be unity) as shown in the top panel of Fig. 5. Such jet onsets are observed in the form of the sporadic formation of parsec-scale components of radio galaxies and quasars (e.g., Zensus et al. 1998). The onset

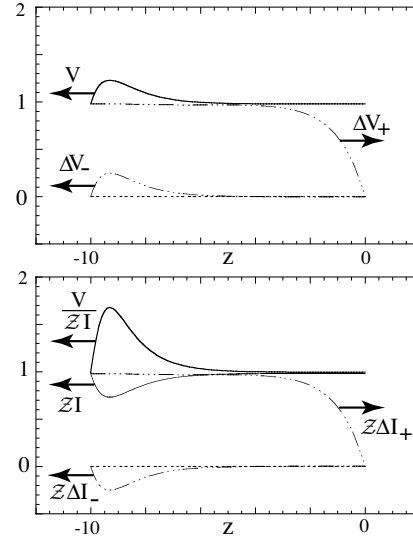


Figure 5. Reflection of an incident wave (ΔV_+ , ΔI_+) off of a stationary load of impedance \mathcal{Z}_L and the reflected wave (ΔV_- , ΔI_-) for the circuit in Fig. 4. The net voltage is $V = \Delta V_+ + \Delta V_-$ and the net current $I = \Delta I_+ + \Delta I_-$. The top panel shows the voltages and the bottom panel the currents as well as the ratio $V/(\mathcal{Z}I)^{-1}$. If this ratio is larger than a critical value, \mathcal{C} (equation 20), then the magnetic insulations will breakdown. For this example, $\mathcal{Z}_L = \mathcal{Z} - i\omega\mathcal{L}$, where \mathcal{L} is the inductance of the load.

may be explained by the global magnetic instability of the disc (Lovelace et al. 1994).

In such cases the wave amplitudes can be written as

$$\Delta V_{\pm}(z, t) = \int_{-\infty}^{\infty} d\omega \Delta V_{\pm}(\omega) \exp[i\omega(\pm z/u_\phi - t)], \quad (21)$$

with $\Delta V_{\pm}(\omega)^* = \Delta V_{\pm}(-\omega)$ and with

$$\Delta V_-(\omega) = \frac{\mathcal{Z}_L - \mathcal{Z}}{\mathcal{Z}_L + \mathcal{Z}} \Delta V_+(\omega) \quad (22)$$

where $\mathcal{Z}_L(\omega)$ is in general frequency-dependent with real and imaginary parts. Figure 5 shows a case where $\mathcal{Z}_L = R - i\omega\mathcal{L}$ is due to a resistance R assumed equal to \mathcal{Z} in series with and inductance \mathcal{L} . An estimate of \mathcal{L} is simply $r_2 L$, where r_2 is the jet radius and L is given by equation (9).

The top panel of Fig. 5 shows that there is a *backward* propagating positive voltage wave ΔV_- . The rise-time of the wave is equal to that of the incident wave while the decay-time is equal to the L over R time of the load. The voltage wave is positive because the inductance of the load appears initially to the incident wave as a high impedance. At the same time the reflected current ΔI_- is negative. The net voltage and current are such that there is a *backward* propagating wave with $V/(\mathcal{Z}I) > \mathcal{C}$. This corresponds to a breakdown of the magnetic insulation.

The condition $V/(\mathcal{Z}I) > \mathcal{C}$ can exist only transiently (for a time $< r_2/c$) because for $E_r < 0$ the insulation breakdown will lead to a radial inflow of positive charge with speed $c(1 - B^2/E^2)^{1/2}$ and an opposite radial outflow of negative charge. At the same time both positive and negative charges drift in the $\mathbf{E} \times \mathbf{B}$ direction with speed $c|B/E|$. This will

bring the transmission line to the threshold condition where $V/(ZI) = C$ or $|\mathbf{E}| = |\mathbf{B}|$.

Both positive and negative charged particles in the region where $|\mathbf{E}| = |\mathbf{B}|$ are accelerated in the $\mathbf{E} \times \mathbf{B}$ direction which is approximately the $+z$ direction. The acceleration is highly efficient in that a particle exposed to the wave for a time Δt is accelerated to a Lorentz factor

$$\gamma_{\mathbf{E} \times \mathbf{B}} \approx 1 + \frac{1}{2} \left(\frac{6eB\Delta t}{mc} \right)^{2/3}, \quad (23)$$

which is much larger than unity. This formula is easily derived from the equations of motion. The electromagnetic energy in the backward propagating wave is dissipated into kinetic energy of the accelerated particles.

As a numerical example relevant to the HST-1 component in M87, we consider $r_2 = 5$ pc and $B = 0.5$ mG (Harris et al. 2009) and assume that the jet consists of electrons and positrons. De Young (2006) discusses different models of extra-galactic jets involving plasmas dominated by electrons and positrons, electrons and ions, and electromagnetic fields (i.e., Poynting flux jets). For the electron-positron case,

$$\gamma_{\mathbf{E} \times \mathbf{B}} \approx 1.2 \times 10^7 \left(\frac{B}{0.5 \text{mG}} \right)^{2/3} \left(\frac{\Delta t}{5 \times 10^8 \text{s}} \right)^{2/3}, \quad (24)$$

where the time Δt is normalized to $r_2/c \approx 5 \times 10^8$ s. The accelerated particles will in a time $\sim r_2/c$ run into the region of the load where the magnetic field has a spread of directions. The L/R time $\sim 5 \times 10^{10}$ s is much longer than the dissipation time for the backward propagating wave. The synchrotron radiation peak from these high- γ leptons is at $\nu_{\text{syn}} = 3eB\gamma^2/2m_e c \approx 3 \times 10^{17}$ Hz or a photon energy ≈ 1300 eV.

If the electromagnetic radiation of the source $\dot{\mathcal{E}}_{\text{rad}}$ is entirely due to the accelerated particles, then $\dot{\mathcal{E}}_{\text{rad}} = \dot{N}_\ell m_e c^2 \gamma_{\mathbf{E} \times \mathbf{B}}$, where N_ℓ is the number of accelerated leptons. Estimating $\dot{N}_\ell \sim \pi r_2^2 c n_\ell$ and taking $\dot{\mathcal{E}}_{\text{rad}} = 10^{42}$ erg/s (Harris et al. 2009) gives the lepton number density $n_\ell \sim 4.5 \times 10^{-9}$ cm $^{-3}$. From this we obtain the so called ‘plasma beta’, $\beta_p = 4\pi n_\ell \gamma_{\mathbf{E} \times \mathbf{B}} m_e c^2 / B^2 \sim 2.2$. This implies that the load region of the jet is *not force-free* and that it will expand. Prior to the acceleration of the particles when the power flow in the jet is unidirectional, $\beta_p = 1.9 \times 10^{-7}$ T so that the jet is dominantly *force-free*. Synchrotron and other losses will give rise to a power law distribution of lepton energies $\propto \gamma^{-q}$ with $q \geq 2$ and with a cutoff at $\gamma_{\mathbf{E} \times \mathbf{B}} m_e c^2$.

The estimated Lorentz factor (24) is larger than a critical value denoted γ_c set by the condition that the inverse Compton scattering of a lepton off a synchrotron photon (energy ε_{syn}), which gives an inverse Compton photon (energy $\varepsilon_{\text{IC}} \approx \gamma^2 \varepsilon_{\text{syn}}$), be such that the subsequent scattering of the synchrotron and secondary inverse Compton photons is above the threshold for electron-positron pair production [$\varepsilon_{\text{syn}} \varepsilon_{\text{IC}} \approx (m_e c^2)^2$]. This condition gives

$$\gamma_c = \left(\frac{2m_e c^2}{3\hbar\omega_c} \right)^{1/3} \approx 3.9 \times 10^5, \quad (25)$$

where $\omega_c = eB/m_e c$ is the non-relativistic cyclotron frequency (e.g., Lovelace 1987). At this Lorentz factor, $\varepsilon_{\text{syn}} = 1.3$ eV and $\varepsilon_{\text{IC}} = 2 \times 10^{11}$ eV.

The acceleration of particles is more complicated in the case of an electron-ion jet. The accelerated electrons will tend to increase $-J_z$ more than the opposite effect from the

ions. This will give rise to an inductive ambipolar E_z field. It in turn retards the electron acceleration and enhances the ion acceleration. However, analysis of this problem is beyond the scope of the present work.

3 CONCLUSIONS

We have developed a model of Poynting jets as a transmission line carrying a net axial current and having a potential drop across it. The currents and voltages are of the order of 3×10^{18} A and $2.7 \times 10^{20} \beta$ V. The energy of ions accelerated across this voltage is large enough to account for ultra high energy cosmic rays (Lovelace 1976; Biermann et al. 2001; Ostrowski 2002). Further, we derive the transmission line impedance and the electromagnetic energy flow in the jet. The observed current in 3C 303 is used to independently estimate the electromagnetic energy flow in this magnetically dominated jet. Time-dependent but not necessarily small perturbations of a Poynting-flux jet - possibly triggered by an irregularity in the jet - are described by the ‘telegraphers’ equations,’ which are wave equations for the current and voltage on the line. The voltage and current consist in general of forward and backward propagating components. The disturbance of a Poynting jet by an irregularity can give rise to localized dissipation in the jet which may explain the enhanced synchrotron radiation in the knots of the 3C 303 jet and in the much smaller apparently stationary knot HST-1.

Lastly, we consider relativistic Poynting jets relevant to parsec-scale jets such as HST-1. The reflected voltage wave from an inductive load (or jet termination) can lead to a backward propagating wave which causes the magnetic insulation to breakdown. That is, it gives $|\mathbf{E}|/|\mathbf{B}| \geq 1$. At the threshold for breakdown, $|\mathbf{E}|/|\mathbf{B}| = 1$, positive and negative particles are directly accelerated in the $\mathbf{E} \times \mathbf{B}$ direction which is approximately along the jet axis. Particles can be accelerated up to Lorentz factors $\sim 10^7$ in a short time interval of the order of the light travel time across the jet. This particle acceleration mechanism is distinct from particle acceleration in shock waves and that in magnetic field reconnection.

The breakdown of magnetic insulation $|\mathbf{E}|/|\mathbf{B}| \geq 1$ is not possible in a plasma that is modeled everywhere by ideal relativistic magnetohydrodynamics (RMHD). This is because the Ohm’s law of RMHD $\mathbf{E} + \mathbf{v} \times \mathbf{B}/c = 0$ requires that $|\mathbf{E}|/|\mathbf{B}| \leq |\mathbf{v}|/c < 1$ everywhere. Of course an actual plasma can readily have $|\mathbf{E}|/|\mathbf{B}| \geq 1$. A common example is magnetic reconnection where there is a region in which the direction of the magnetic field reverses so that $|\mathbf{B}|$ goes through zero on a surface. But even in regions of non-zero $|\mathbf{B}|$ a plasma can have $|\mathbf{E}|/|\mathbf{B}| \geq 1$ transiently as in pulse propagation along magnetically insulated transmission lines (e.g., Shope et al. 1978; Samokhin 2010). The restrictive Ohm’s law constraint of RMHD can be avoided in relativistic-electromagnetic particle-in-cell simulations where the orbits of individual particles are calculated (e.g., Lovelace, Gandhi, & Romanova 2005).f

An open question regarding the propagation of relativistic current-carrying Poynting jets is the kink instability. In the context of laboratory current-carrying plasmas, the kink instability is predicted and observed to occur if the current

is larger than a critical value which is the Kruskal-Shafranov condition (e.g., Kadomtsev 1966; Huarte-Espinosa et al. 2012). The theory of the instability for relativistic Poynting jets has not been developed. Observational evidence for large current flows in astrophysical jets (e.g., Kronberg et al. 2011) suggest that the jets can withstand the kink instability. On the other hand a mechanism for the nonlinear stabilization of the kink instability was proposed by Kadomtsev (1966, p. 188).

ACKNOWLEDGMENTS:

We thank D.E. Harris, G.S. Bisnovaty-Kogan, S. Dyda, and M.M. Romanova for valuable discussions. Also, we thank the referee for valuable criticism. RVEL was supported in part by NASA grants NNX10AF-63G and NNX11AF33G and by NSF grant AST-1008636. PPK acknowledges support from NSERC Canada Discovery Grant A5713.

REFERENCES

- Asada, K., Inoue, M., Kamenno, S., Fujisawa, K., Iguchi, S., & Mutoh, M. 2002, PASJ, 54, L39
- Beckwith, K., Hawley, J.F., & Krolik, J.H. 2008, ApJ, 678, 1180
- Benford, G. 1978, MNRAS, 183, 29
- Bergeron, K.D. 1977, J. of Applied Phys., 48, 3065
- Biermann, P.L., Kang, H., & Ryu, D. 2001, in ASP Conf. Series, V. 241, 57
- Biretta, J.A., Sparks, W.B., & Macchetto, F. 1999, ApJ, 520, 621
- Bisnovaty-Kogan, G.S., & Lovelace, R.V.E. 1995, A&A, 296, L17
- Blandford, R.D., & Znajek, R.L. 1977, MNRAS, 179, 433
- De Young, D.S. 2006, ApJ, 648, 200
- Gabuzda, D.C., Murray, E., & Cronin, P. 2004, MNRAS, 351, L89
- Gordeev, A.V. 1978, Sov. Phys. Tech. Phys., 23, 463
- Harris, D.E., Cheung, C.C., Stawarz, L., Biretta, J.A., & Perlman, E.S. 2009, ApJ, 699, 305
- Heaviside, O. 1893, *Electromagnetic Theory*, (D. Van Nostrand: New York), p. 449
- Huarte-Espinosa, M., Frank, A., Blackman, E.G., Ciardi, A., Hartigan, P., Lebedev, S.V., & Chittenden, J.P. 2012, ApJ, 757: id.=66
- Kadomtsev, B.B. 1966, in *Reviews of Plasma Physics*, V. 2, pp. 153
- Kronberg, P.P., Dufton, Q. W., Li, H., & Colgate, S. A. 2001, ApJ, 560, 178
- Kronberg, P.P., Lovelace, R.V.E., Lapenta, G. & Colgate, S.A. 2011, ApJ, 741, L15
- Lovelace, R.V.E. & Ott, E. 1974, Phys. of Fluids, 17, 1263
- Lovelace, R.V.E. 1976, Nature, 262, 649
- Lovelace, R.V.E. 1987, A&A, 173, 237
- Lovelace, R.V.E., Wang, J.C.L., & Sulkanen, M.E. 1987, ApJ, 315, 504
- Lovelace, R.V.E., Romanova, M.M., & Newman, W.I. 1994, ApJ, 437, 136
- Lovelace, R.V.E., Li, H., Koldoba, A.V., Ustyugova, G.V., & Romanova, M.M. 2002, ApJ, 572, 445
- Lovelace, R.V.E., & Romanova, M.M. 2003, ApJ, 596, L162
- Lovelace, R.V.E., Gandhi, P.R., & Romanova, M.M. 2005, Ap&SS 298, 115
- Li, H., Lovelace, R.V.E., J. M. Finn, J.M., & Colgate, S.A. 2001, ApJ, 561, 915
- Lynden-Bell, D. 1996, MNRAS, 279, 389
- McKinney, R.D. 2006, MNRAS, 368, 1561

- Nakamura, M., Tregillis, I.L., Li, H., & Li, S. 2008, ApJ, 686, 843
- Ostrowski, M. 2002, *Astroparticle Physics* 18, 229
- Ron, A., Mondelli, A.A., & Rostoker, N. 1973, IEEE Trans. Plasma Sci. PS-1, 85
- Samokhin, A.A. 2010, Plasma Phys. Reports, 36, 682
- Shope, S., Poukey, J.W., Bergeron, K.D., MacDaniel, D.H. Toepfer, A.J., & Vandevender, J.P. 1978, J. of Applied Phys., 49, 3675
- Tchekhovskoy, A., Narayan, R., & McKinney, J.C. 2011, MNRAS, 418, L79
- Ustyugova, G.V., Lovelace, R.V.E., Romanova, M.M., Li, H., & Colgate, S.A. 2000, ApJ, 541, L21
- Zavala, R.T., & Taylor, G.B. 2005, ApJ, 626, L73
- Zensus, J.A., Taylor, G.B., & Wrobel, J.M. (eds.) 1998, *Radio Emission from Galactic and Extragalactic Compact Sources*, IAU Colloquium 164, (Astronomical Society of the Pacific: San Francisco)

APPENDIX A: WAVEGUIDE MODEL OF POYNTING JET

There are a wide range of axisymmetric, translationally-symmetric, time-independent Poynting jet models which satisfy the relativistic, force-free equation,

$$\frac{dB_z^2}{dr} + \frac{1}{r^2} \frac{d[r^2(B_\phi^2 - E_r^2)]}{dr} = 0, \quad (\text{A1})$$

(cgs units). This assumes that there is plasma everywhere, but that the ‘plasma beta’ - the ratio of the kinetic energy-density to electromagnetic field energy-density is $\ll 1$. The time-independence of the solutions of (A1) implies that the energy flow in the jet is *unidirectional*. Here, we assume this is the $+z$ direction. Realistic models can in principle be derived for example from relativistic particle-in-cell simulations (e.g., Lovelace et al. 2005). Here, we discuss a waveguide-like jet model alternative to that considered in the text. The electric and magnetic fields are similar to the fields in a TEM coaxial waveguide. This model is suggested by the work of Bisnovaty-Kogan & Lovelace (1995).

Equation (A1) is satisfied by the fields shown in Fig. A1. For $r < r_1$, the magnetic field is $B_z = \text{const}$ and the electric field is zero. For $r_1 < r < r_2$, the magnetic field is $B_\phi = -B_0(r_1/r) < 0$, and the electric field is $E_r = \eta B_\phi < 0$ where $B_0 = (1 - \eta^2)^{-1/2} B_z$, and $\eta = \text{const} < 1$ is dimensionless (cgs units). For $r_2 < r < r_3$, the magnetic field is $B_\phi = (1 - \eta^2)^{1/2} B_0(r_1/r)$ and the electric field is zero. The condition on the magnetic field at r_3 is the same as discussed in the text. The plasma in the region $r_1 < r < r_2$ has a uniform axial $\mathbf{E} \times \mathbf{B}$ drift velocity $\eta c \hat{\mathbf{z}}$ or Lorentz factor $\Gamma = (1 - \eta^2)^{-1/2}$. This model involves only a small number of parameters, (r_1, r_2, B_0, η).

In MKS units, the current carried by the core of the jet (in A) is $I_0 = 2\pi r_1 B_0 / \mu_0$. Thus the poloidal flux carried by the jet is

$$\Phi_z = \pi r_1^2 B_z = \frac{1}{2} (1 - \eta^2)^{1/2} \mu_0 r_1 I_0. \quad (\text{A2})$$

The voltage drop across the jet is

$$V_0 = - \int_{r_1}^{r_2} dr E_r = Z_0 I, \quad (\text{A3})$$

where

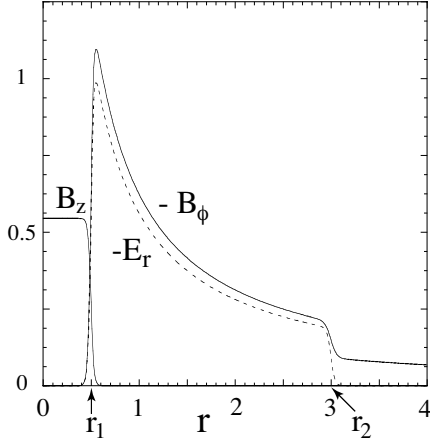


Figure A1. Field profiles of a Poynting jet model alternative to that of the text (eqn. 2 and Fig. 2). Here, we have taken $\eta = 0.9$, $r_1 = 0.5$ with a narrow boundary layer, and $r_2 = 3$ also with a narrow boundary layer.

$$\mathcal{Z}_0 = \frac{1}{2\pi} \sqrt{\frac{\mu_0}{\epsilon_0}} \eta \ln\left(\frac{r_2}{r_1}\right) = 60 \eta \ln\left(\frac{r_2}{r_1}\right) \Omega \text{ [MKS]}. \quad (\text{A4})$$

This formula is the counterpart of equation (4). The electromagnetic power flow in the Poynting jet is

$$\dot{E}_j = \frac{2\pi}{\mu_0} \int_{r_1}^{r_2} r dr E_r B_\phi = \mathcal{Z}_0 I_0^2, \quad (\text{A5})$$

which agrees with the equation (3).

The electric field energy per unit length is

$$w_E = \frac{\epsilon_0}{2} 2\pi \int_{r_1}^{r_2} r dr E_r^2 = \frac{1}{2} C V_0^2, \quad (\text{A6})$$

where

$$C = \frac{2\pi\epsilon_0}{\ln(r_2/r_1)} \quad (\text{A7})$$

is the capacitance per unit length of the jet.

The magnetic energy per unit length of the jet is

$$\begin{aligned} w_B &= \frac{\pi}{\mu_0} \int_0^{r_1} r dr B_z^2 + \frac{\pi}{\mu_0} \int_{r_1}^{r_2} r dr B_\phi^2, \\ &= \frac{1}{2} L I_0^2. \end{aligned} \quad (\text{A8})$$

Carrying out the integrals we find

$$L = \frac{\mu_0}{2\pi} \left[\frac{1-\eta^2}{2} + \ln\left(\frac{r_2}{r_1}\right) + (1-\eta^2) \ln\left(\frac{r_3}{r_2}\right) \right], \quad (\text{A9})$$

which is the inductance per unit length of the jet.

From equations (A7) and (A9) we find the wave speed on the jet is

$$u_\varphi = c \left(1 + \frac{1-\eta^2}{2 \ln(r_2/r_1)} + \frac{(1-\eta^2) \ln(r_3/r_2)}{\ln(r_2/r_1)} \right)^{-1/2}, \quad (\text{A10})$$

The wave impedance of the transmission line is

$$\mathcal{Z} = \mathcal{Z}_0 \left(1 + \frac{1-\eta^2}{2 \ln(r_2/r_1)} + \frac{(1-\eta^2) \ln(r_3/r_2)}{\ln(r_2/r_1)} \right)^{1/2}. \quad (\text{A11})$$

Equations (A10) and (A11) are the analogues of equations (12) and (14).